# GENERAL GREEN'S FUNCTIONS METHOD FOR THERMOACOUSTIC GENERATION IN ANISOTROPIC ORGANIC CONDUCTORS

BILJANA MITRESKA, DANICA KRSTOVSKA†

Ss. Cyril and Methodius University, Faculty of Natural Sciences and Mathematics,
Arhimedova 3, 1000 Skopje, Macedonia
Corresponding author†: danica@pmf.ukim.mk, krstovska@magnet.fsu.edu

*Received June 2, 2018*

*Abstract*. The thermoacoustic generation in anisotropic layered organic conductors was considered using Green's functions method to solve the equation for temperature distribution and the acoustic wave equation. The proposed method was demonstrated by applying a heat current as a thermal source at the conductor's surface. The corresponding expressions for the temperature distribution and acoustic wave amplitude are obtained in the case of low temperature when the depth of thermal skin layer is substantially larger than the depth of electromagnetic skin layer. The thermoacoustic generation is studied in detail for the simplest dispersion relation for the quasi-two dimensional charge carriers which, in many cases, allows a correct understanding of the electron transport and dynamics in layered organic conductors. The diversity of the phenomenon studied through its angular and magnetic field dependence is reflected in a number of features which provide a rich material for studying the properties of charge carriers in low dimensional conducting systems under the influence of different thermal and mechanical conditions.

*Key words*: Thermoacoustic generation, quasi-two dimensional organic conductors, Green's functions, thermal and mechanical boundary, semiclassical calculations, ultrasonics.

*PACS*: 72.15.Eb, 72.15.Jf, 43.20.+g, 74.70.Kn.

## 1. INTRODUCTION

It has long been known that a modulated thermal source may be used to create acoustic waves. The basic principle of thermoacoustic generation within a solid involves the coupling of energy from thermal expansion and contraction into an acoustic wave. The acoustic process identified by selected characteristics can be a source of information about state of material, its structure, and properties, which is particularly important for systems exhibiting anisotropy properties, and such are layered organic conductors. Organic conductors, being characterized by an extremely high electronic anisotropy, rather simple Fermi surface (FS), and high crystal quality, are excellent objects for studying general properties of quasi-two-dimensional (q2D) metallic systems. In particular, their behaviour in strong magnetic fields is found to be qualitatively different from that of usual three-dimensional metals or purely

two-dimensional systems [1]. Due to the reduced dimensionality and relatively low carrier concentrations, many organic conductors exhibit strong electron correlations and, consequently, numerous instabilities of the normal metallic state.

In layered organic conductors, linear thermoacoustic generation has been considered in those with only q2D group of charge carriers [2]. These include the series of q2D organic conductors $\beta-(\mathrm{BEDT-TTF})_2\mathrm{X}$ (where BEDT-TTF denotes bis(ethylenedithio)tetrathiafulvalene and X=$IBr_2$, $I_3$, $I_2Br$) whose FS consists of a corrugated cylinder open in the direction of the normal with respect to the layers. Later, the research was extended to thermoacoustic generation conditioned by the Nernst effect in organic conductors with two conducting channels, quasi-one dimensional (q1D) and q2D [3]. Such are the series of q2D organic conductors $\alpha-(\mathrm{BEDT-TTF})_2\mathrm{MHg(SCN)}_4$ (M=K, $\mathrm{NH}_4$, Rb and Tl) which have attracted considerable attention over the last few years due to two different ground states and rich phenomena associated with them. These are isostructural layered charge-transfer salts with the FS comprising a pair of slightly warped open sheets (representing a q1D conduction band) and a cylinder (a q2D band). Recently, the nonlinear thermoacoustic generation due to Joule heating as a heat source in layered q2D organic conductors was studied [4]. In that case, only a second harmonic wave is generated due to the thermoelectric stresses caused by the alternating part of the Joule heat. Usually the problem of thermoacoustic generation in conducting media is studied by solving analytically a set of equations that concise of several partial differential equations (PDEs) including Maxwell's equations for the magnetic $\mathbf{B}$ and electric $\mathbf{E}$ field, the thermal conduction equation that describes the propagation of the acoustic wave with the presence of a heat flux $\mathbf{q}$ and/or a heat source $Q_h$ and the acoustic wave equation for ionic displacement $\mathbf{U}$ that takes into account the thermoelectric stress tensor arising from the nonuniform temperature oscillations.

In this paper, a more general approach is used for solving the problem of thermoacoustic generation in anisotropic organic conductors by employing the Green's functions method to solve the thermal conduction equation and acoustic wave equation in presence of an arbitrary heat source at the conductor's surface. The solutions for the temperature distribution and the acoustic wave amplitude are expressed in an integral form which may be solved analytically and numerically by using an appropriate expression for the heat source causing the temperature and hence acoustic oscillations within the conductor.

## 2. GREEN'S FUNCTIONS APPROACH FOR THERMOACOUSTIC GENERATION IN PRESENCE OF A SURFACE HEAT SOURCE

In the process of thermoacoustic generation a given surface heat source at frequency $\omega$ induces nonuniform temperature oscillations of the same frequency. These

oscillations, in turn, generate longitudinal acoustic oscillations in the conductor with a frequency that coincides with the frequency of the heat source. We consider the case when a heat source, for example, a heat current with frequency $\omega$, $J_z^T \sim e^{-i\omega t}$, is flowing through the conductor along the least conducting axis of the conductor ($z-$ axis), *i.e.*, along the direction with the greatest resistance. The thermoacoustic generation is manifested under the conditions of the normal skin effect, when the electron mean-free path length $l$ is much smaller than the penetration depth of both the electromagnetic $\delta_E$ and thermal field $\delta_T$ in the conductor, $l \ll \delta_E, \delta_T$. We consider thermoacoustic generation at low temperatures when the thermal skin depth $\delta_T$ is much larger than the electromagnetic one, $\delta_T \gg \delta_E$. A temperature oscillating with the same frequency $\omega$ as the heat source ($\Theta \sim e^{-i\omega t}$) can occur if $\omega\tau \ll 1$ where $\tau$ is the relaxation time of the conduction electrons. In this case the condition for normal skin effect is satisfied automatically as $l/\delta_T \approx \sqrt{\omega\tau} \ll 1$. The temperature oscillations generate thermoelectric stresses which induce only longitudinal acoustic waves and therefore all of the quantities depend only on the $z$ component.

In this section the thermal conduction equation and acoustic wave equation will be solved by applying the traditional method of Green's functions. The solutions will be presented in an integral form for two distinct thermal conditions at the conductor's surface-isothermal and adiabatic as well as two mechanical conditions-fixed and free boundary.

### 2.1. INTEGRAL FORM FOR THE TEMPERATURE DISTRIBUTION FUNCTION $\Theta(z)$

In order to calculate the amplitude of the generated acoustic waves we first have to determine the temperature distribution within the conductor resulting from the surface heat source. Consequently, we have to solve the thermal conduction equation which includes the heat flux arising from the arbitrary heat source $Q_h$

$$\frac{\partial^2\Theta}{\partial z^2} + k_T^2\Theta = \frac{dQ_h}{dz}, \tag{1}$$

where the thermal wave number $k_T$ and skin depth $\delta_T$ are given as

$$k_T = \frac{1+i}{\delta_T}, \quad \delta_T = \sqrt{\frac{2\kappa_{zz}}{\omega C}}, \tag{2}$$

and $Q_h$ is defined as

$$Q_h(z) = \frac{J_z^T}{\kappa_{zz}}. \tag{3}$$

Here $J_z^T$ is the power density of the surface heat source due to the thermoelectric effect, $\kappa_{zz}$ is the thermal conductivity tensor, $C$ is the volumetric heat capacity.

### 2.1.1. Isothermal boundary condition

The isothermal boundary condition requires that the temperature oscillations vanish at the surface $z = 0$

$$\Theta_I(z)|_{z=0} = 0. \tag{4}$$

The general solution of eq. (1) expressed in terms of Green's function $G(z,\xi)$ is given as

$$\Theta(z) = \int_0^\infty G(z,\xi)\frac{dQ_h}{dz}|_{z=\xi}d\xi. \tag{5}$$

Since the Green function is the solution of the homogeneous differential equation for the temperature conduction equation we obtain the following solutions

$$G_1(z,\xi) = A_1e^{ik_Tz} + B_1e^{-ik_Tz}, \quad G_2(z,\xi) = A_2e^{ik_Tz} + B_2e^{-ik_Tz}. \tag{6}$$

By using the isothermal boundary condition and demanding the function to be finite in infinity

$$G_1(0,\xi) = 0, \;\; G_2(\infty,\xi) = 0, \tag{7}$$

the Green functions take the form

$$G_1(z,\xi) = A_1e^{ik_Tz} + B_1e^{-ik_Tz}, \quad G_2(z,\xi) = A_2e^{ik_Tz}. \tag{8}$$

Using the boundary conditions (7) and the two standard conditions for the Green function that involve the continuity and jump at $z = \xi$

$$G_1(z,\xi)|_{z=\xi} = G_2(z,\xi)|_{z=\xi}, \tag{9}$$

$$\frac{dG_2(z,\xi)}{dz}|_{z=\xi} - \frac{dG_1(z,\xi)}{dz}|_{z=\xi} = 1, \tag{10}$$

the following expressions for the constants $A_1, B_1$ and $A_2$ are obtained

$$A_1 = -B_1 = -\frac{1}{2ik_T}e^{ik_T\xi}, \quad A_2 = -\frac{1}{2ik_T}\Big(e^{ik_T\xi} - e^{-ik_T\xi}\Big). \tag{11}$$

Substituting the Green's functions in the eq. (5) the expression for the temperature distribution is written in the following form

$$\Theta_I(z) = -\frac{1}{k_T}\Big(e^{ik_Tz}\int_0^z \sin(k_T\xi)\frac{dQ_h}{dz}\Big|_{z=\xi}d\xi + \sin(k_Tz)\int_z^\infty e^{ik_T\xi}\frac{dQ_h}{dz}\Big|_{z=\xi}d\xi\Big). \tag{12}$$

We consider low temperature thermal generation of bulk acoustic waves, *i.e.*, at large distance from the conductor's surface, $z \gg \delta_h$, where $\delta_h$ is the penetration depth of the heat source $Q_h(z)$. In that case it is sufficient to take into account only the first term in eq. (12) where the upper limit in the integral is replaced with $\infty$. An expansion in power series of $k_T\xi$ up to the first non-vanishing term transforms eq. (12)

into the following expression for the temperature distribution in case of an isothermal boundary

$$\Theta_I(z) = e^{ik_T z} \int_0^\infty Q_h(\xi) d\xi. \tag{13}$$

### 2.1.2. Adiabatic boundary condition

The adiabatic boundary condition requires that there is no heat flux through the conductor's surface

$$\frac{d\Theta_A}{dz}|_{z=0} = 0. \tag{14}$$

Again, applying the Green functions method by using the same Green functions as above, eq. (6), and the accompanying in this case conditions for the Green function

$$\frac{dG_1(0,\xi)}{d\xi} = 0, \;\; G_2(\infty,\xi) = 0, \tag{15}$$

one obtains the following relations for the corresponding constants

$$A_1 = B_1 = \frac{1}{2ik_T} e^{ik_T\xi}, \quad A_2 = \frac{1}{2ik_T}(e^{ik_T\xi} + e^{-ik_T\xi}). \tag{16}$$

The temperature distribution for the adiabatic boundary is represented as follows

$$\Theta_A(z) = -\frac{i}{k_T}\Big(e^{ik_T z}\int_0^z \cos(k_T\xi)\frac{dQ_h}{dz}\Big|_{z=\xi} d\xi + \cos(k_T z)\int_z^\infty e^{ik_T\xi}\frac{dQ_h}{dz}\Big|_{z=\xi} d\xi\Big). \tag{17}$$

As in the case of an isothermal boundary, expanding the first term in powers of $k_T\xi$ up to the first non-vanishing term and changing the upper limit of the integral to $\infty$ the following expression for the temperature distribution is obtained

$$\Theta_A(z) = -ik_T e^{ik_T z}\int_0^\infty \xi Q_h(\xi) d\xi. \tag{18}$$

## 2.2. INTEGRAL FORM FOR THE ACOUSTIC WAVE AMPLITUDE $U_\omega^{I,A}$

To calculate the amplitude of the generated acoustic wave it is necessary to solve the acoustic wave equation. Since we consider a case when the heat source and the induced temperature oscillations are along the less conducting axis, $z-$axis of the conductor, the generated acoustic wave is longitudinal. In that case the acoustic wave equation is written in the following form

$$\frac{\partial^2 U_\omega(z)}{\partial z^2} + q^2 U_\omega(z) = \beta\frac{d\Theta}{dz}, \tag{19}$$

where $q = \omega/s$ is the wave vector, $s$ is the acoustic wave velocity, $\beta$ is the volumetric expansion coefficient. The term $\beta d\Theta/dz$ takes into account the thermoelectric

stresses arising from the nonuniform temperature oscillations that generate acoustic oscillations.

Procedures for obtaining the integral form of the acoustic wave equation solution are performed in the same manner as for the thermal conduction equation by using the expression that defines the wave amplitude

$$U_\omega(z) = \beta \int_0^\infty G(z,\xi) \frac{d\Theta}{dz}|_{z=\xi} d\xi, \tag{20}$$

and the corresponding Green functions in the form

$$G_1(z,\xi) = A_1 e^{iqz} + B_1 e^{-iqz}, \quad G_2(z,\xi) = A_2 e^{iqz}. \tag{21}$$

When performing experiments on thermoacoustic generation efficiency or amplitude of the generated wave the boundary significantly affects their properties. Therefore, for experimental purposes it is useful to specify the type of the boundary in order to correctly estimate and explain the experimental data. In the following we shall consider two types of mechanical boundary, fixed (contact generation of acoustic waves) and free (contactless generation of acoustic waves) boundary in order to analyse the behaviour of the thermally generated waves (isothermal and adiabatic case) in case of different boundary conditions. In addition, we can determine if there is a preference of one type of boundary over another and how it is reflected on the magnetic field and angular dependence of the acoustic wave amplitude.

### 2.2.1. Fixed boundary condition

The fixed boundary condition requires that the wave amplitude vanishes at the conductor's surface

$$U_\omega^{I,A}(z)|_{z=0} = 0. \tag{22}$$

The solution for the acoustic wave amplitude in the case of an isothermal and fixed mechanical boundary takes the following integral form

$$U_\omega^I = \beta \int_0^\infty \Theta_I(\xi) d\xi. \tag{23}$$

Since in the case of a fixed adiabatic boundary $\int_0^\infty \Theta_A(\xi) d\xi = 0$ (there is no heat flux through the adiabatic boundary) we have to take into account the quadratic term in the expansion in powers of $q\xi$. In that case the integral form for the acoustic wave amplitude is given as

$$U_\omega^A = -\frac{\beta q^2}{2} \int_0^\infty \xi^2 \Theta_A(\xi) d\xi. \tag{24}$$

### 2.2.2. Free boundary condition

By making use of a free and isothermal boundary condition for the acoustic wave amplitude

$$\frac{dU_\omega^I(z)}{dz}|_{z=0} = 0, \tag{25}$$

and solving the acoustic wave equation by using the Green's functions method we obtain the following expression for the wave amplitude

$$U_\omega^I = -iq\beta \int_0^\infty \xi\Theta_I(\xi)d\xi. \tag{26}$$

On the other hand, the adiabatic thermal condition in case of a free mechanical boundary requires that

$$\frac{dU_\omega^A(z)}{dz}|_{z=0} = \beta\Theta_A|_{z=0}, \tag{27}$$

and provides the following integral solution for the acoustic wave amplitude

$$U_\omega^A = -i\frac{\beta}{q}\int_0^\infty \frac{d\Theta_A}{dz}\Big|_{z=\xi} d\xi - iq\beta\int_0^\infty \xi\Theta_A(\xi)d\xi. \tag{28}$$

## 3. CALCULATIONS OF THE ACOUSTIC WAVE AMPLITUDE FOR A SPECIFIC SURFACE HEAT SOURCE

The amplitude of the generated wave is a function of the characteristics of the conductor: electrical conductivity $\sigma_{ij}$, thermoelectric coefficient $\alpha_{ij}$ and thermal conductivity $\kappa_{ij}$. Once the transport coefficients are calculated the acoustic wave amplitude can be determined applying the corresponding integral forms obtained by the Green's functions method for a given heat source at the conductor's surface. Transport phenomena are usually studied under the linear response approximation so that we only consider the linear term proportional to the external perturbation, *e.g.* electric current **j**. Defining the heat source is a heat current of frequency $\omega = 10^8 - 10^9$ Hz flowing along the $z-$axis of the conductor

$$J_z^T = k_B T\alpha_{zx} j_x, \qquad j_x = \frac{ik_E^2}{\omega\mu_0} e^{i(k_E z-\omega t)}, \tag{29}$$

where electromagnetic wave number $k_E$ and skin depth $\delta_E$ are given as

$$k_E = \frac{1+i}{\delta_E}, \quad \delta_E = \sqrt{\frac{2}{\omega\mu_0\sigma_{xx}}}, \tag{30}$$

$k_B$ is the Boltzmann constant, $T$ is the equilibrium temperature of the crystal, $\mu_0$ is the magnetic permeability of the vacuum, $\alpha_{zx}$ is the thermoelectric coefficient tensor component and $j_x$ is the current density determined from the Maxwell's equations

for a magnetic field oriented at angle $\theta$ in the $xz$ plane, $\mathbf{B} = (B\sin\theta, 0, B\cos\theta)$. This yields the following expression for $Q_h(z)$ in the thermal conduction equation

$$Q_h(z) = i\frac{k_B T \alpha_{zx}}{\omega \mu_0 \kappa_{zz}} k_E^2 e^{ik_E z}. \tag{31}$$

Substituting eq. (31) into eqs. (13) and (18) we obtain the temperature distribution for the isothermal and adiabatic thermal condition, respectively

$$\Theta_I(z) = -\frac{k_B T \alpha_{zx}}{\omega \mu_0 \kappa_{zz}} k_E e^{ik_T z}, \quad \Theta_A(z) = -\frac{k_B T \alpha_{zx}}{\omega \mu_0 \kappa_{zz}} k_T e^{ik_T z}. \tag{32}$$

In the following we make use of the integral solutions for the acoustic wave amplitude in order to obtain the corresponding expressions for the two mechanical boundaries.

Using eqs. (32) and the integral form for the wave amplitude in the case of a fixed isothermal and adiabatic boundary (eqs. (23) and (24)) the following expressions are obtained

$$U_\omega^I = -i\beta \frac{k_B T \alpha_{zx}}{\omega} \sqrt{\frac{\sigma_{xx}}{\mu_0 \kappa_{zz} C}}, \quad U_\omega^A = -\beta q^2 \frac{k_B T \alpha_{zx}}{\omega^2 \mu_0 C}. \tag{33}$$

Similarly, we present the expressions for the wave amplitude in the case of a free isothermal and adiabatic boundary, respectively

$$U_\omega^I = (1+i) q \beta \frac{k_B T \alpha_{zx}}{C} \sqrt{\frac{\sigma_{xx}}{2\omega^3 \mu_0}}, \tag{34}$$

$$U_\omega^A = (i-1)\frac{\beta}{q} \frac{k_B T \alpha_{zx}}{\mu_0 \kappa_{zz}} \sqrt{\frac{C}{2\omega \kappa_{zz}}} - (1+i) q \beta \frac{k_B T \alpha_{zx}}{\mu_0} \sqrt{\frac{1}{2\kappa_{zz}\omega^3 C}}. \tag{35}$$

### 3.1. DETERMINATION OF THE TRANSPORT COEFFICIENTS

Considering a q2D electronic band model the transport coefficients $\sigma_{xx}$, $\alpha_{zx}$ and $\kappa_{zz}$ can be calculated by using the linearised semiclassical Boltzmann equation [5]. We assume that the FS consists of a corrugated cylinder extending along $k_z$ and represent the q2D electronic band by the following dispersion relation derived from a tight-binding model

$$\varepsilon(\mathbf{k}) = \frac{\hbar^2}{2m^*}(k_x^2 + k_y^2) - 2t_c \cos(ck_z). \tag{36}$$

Here $\mathbf{k} = (k_x, k_y, k_z)$ is the electron wavevector, $c$ is the distance between the conducting layers, $t_c$ is the interlayer transfer integral, $\hbar$ is Planck's constant divided by $2\pi$ and $m^*$ is the charge carrier effective mass.

Based on the band model eq. (36), the acoustic wave amplitude can be calculated by using the linearised Boltzmann equation and corresponding integral solutions for the wave amplitudes obtained above by the Green's functions method. We

must first calculate the conductivity tensor components using the Boltzmann transport equation

$$\sigma_{ij} = \frac{e^2\tau}{4\pi^3}\int d\mathbf{k^3}\Big(-\frac{\partial f_0(\varepsilon)}{\partial\varepsilon}\Big)v_i(\mathbf{k},0)\int_{-\infty}^{0} v_j(\mathbf{k},t)e^{t/\tau}dt. \tag{37}$$

where $\sigma_{ij}$ is a component of the conductivity tensor, $e$ is the electron charge, $f_0(\varepsilon)$ is the unperturbed quasiparticle (Fermi-Dirac) distribution function, $v_i$ and $v_j$ are velocity components in $\mathbf{k}$ space, and $1/\tau$ is the $\mathbf{k}$-independent scattering rate.

We restrict our considerations to the case when $t_c \ll \mu$ which corresponds to a weak FS corrugation limit. Additionally, in the low temperature limit $-\frac{\partial f_0(\varepsilon)}{\partial\varepsilon} \simeq \delta(\varepsilon-\mu)$ so that the motion of electrons affecting the transport is restricted to the FS. Applying the Boltzmann equation the expression for the interlayer electrical conductivity $\sigma_{zz}$ can be written in the following simplified form

$$\sigma_{zz} = \frac{2e^2\tau m^*}{(2\pi\hbar)^2}\int_0^{\frac{2\pi\cos\theta}{c}} dk_B\bar{v}_z^2. \tag{38}$$

Here $k_B = (k_x\sin\theta + k_z\cos\theta)/\hbar = \text{const}$ is the electron wavevector component along the magnetic field $\mathbf{B}$.

The time-averaged interlayer velocity $\bar{v}_z$ is then given by the following expression, (using the energy dispersion law (eq. (36)))

$$\bar{v}_z = \frac{2ct_c}{\hbar}\sin\Big(\frac{ck_B}{\cos\theta} - ck_F\tan\theta\Big), \tag{39}$$

where $k_F$ is the magnitude of the Fermi wavevector.

By substituting the eq. (39) in the eq. (38) the following expression for the interlayer electrical conductivity $\sigma_{zz}$ is obtained

$$\sigma_{zz} = \sigma_0\left\{J_0^2(ck_F\tan\theta) + \frac{2h^2}{B^2}(1+\tan^2\theta)\sum_{k=1}^{\infty}\frac{J_k^2(ck_F\tan\theta)}{\frac{h^2}{B^2}(1+\tan^2\theta)+k^2}\right\}. \tag{40}$$

Here $\sigma_0$ is the electrical conductivity in the plane of the layers in absence of a magnetic field, $h = m^*/e\tau$ and $J_k$ is the k-order Bessel function.

After averaging the equation of motion $\frac{\partial k_y}{\partial t} = e\mu_0 B\cos\theta(v_z\tan\theta - v_x)/\hbar$ over a sufficiently long time interval about the order of the mean free time of electrons, one obtains the relation for the time-averaged in-plane electron velocity $\bar{v}_x$ of q2D charge carriers, $\bar{v}_x = v_F + \bar{v}_z\tan\theta$, where $v_F$ is the Fermi velocity of electrons. This allows to calculate the transport coefficients that describe the in-plane conductivity in the following form

$$\sigma_{xx} = \frac{h^2\sigma_0}{B^2} + \Big(\frac{h^2\sigma_0}{B^2} + \sigma_{zz}\Big)\tan^2\theta, \quad \sigma_{zx} = \frac{h\sigma_0}{B}\sqrt{1+\tan^2\theta} + \sigma_{zz}\tan\theta. \tag{41}$$

The thermoelectric coefficient tensor components $\alpha_{ij}$ can be expressed using the

Mott formula $\alpha_{ij} = \frac{\pi^2 k_B T}{3e} \frac{d\sigma_{ij}(\varepsilon)}{d\varepsilon} \mid_{\varepsilon=\mu}$, where $\mu$ is the chemical potential of the electron system. The $\alpha_{zx}$ component is written in the following form

$$\alpha_{zx} = \frac{\pi^2 k_B T}{3e} \frac{\sigma_0}{\mu} \tan\theta \Bigg\{ -2J_0(ck_F \tan\theta) J_1(ck_F \tan\theta) + \\ + \frac{2h^2}{B^2}(1+\tan^2\theta) \sum_{k=1}^{\infty} \frac{J_k(ck_F \tan\theta)\Big(J_{-k+1}(ck_F \tan\theta) - J_{k+1}(ck_F \tan\theta)\Big)}{\frac{h^2}{B^2}(1+\tan^2\theta) + k^2} \Bigg\}. \tag{42}$$

The thermal conductivity tensor components are easily calculated since according to the Wiedemann-Franz law for elastic electron scattering the thermal conductivity is proportional to electrical conductivity, $\kappa_{ij} \propto \sigma_{ij}(\varepsilon)$. The $\kappa_{zz}$ component is then given as follows

$$\kappa_{zz} = \frac{\pi^2 k_B^2 T}{3e^2} \sigma_{zz}. \tag{43}$$

## 4. RESULTS AND DISCUSSION

In this section we will consider the behaviour of thermally generated acoustic waves associated with a FS in the form of a cylinder slightly warped along the $z-$axis. Such a FS is, for example, typical of salts with the $\beta$-type packing of organic cation radicals. In particular, $\beta-(\mathrm{BEDT-TTF})_2\mathrm{IBr}_2$ appeared to be an ideal model object demonstrating all the basic effects. We will start with the most remarkable phenomenon in organic conductors, angle-dependent acoustic wave oscillations, which could provide additional information about the electronic system. We will also consider the behaviour of the acoustic wave amplitude with the magnetic field strength specifically when the field is rotated at the peaks (maximum wave amplitude) and dips (minimum wave amplitude) in the angular dependence.

Below a detailed description of the evolution of thermally generated bulk acoustic waves ($\omega = 10^8 - 10^9$ Hz) with magnetic field strength and its orientation is presented using the parameter values for $\beta-(\mathrm{BEDT-TTF})_2\mathrm{IBr}_2$: $t_c = 0.35$ meV, $m^* = 4.2m_e$, $\tau = 10$ ps and $\mu \sim 0.1$ eV [1]. The value of the parameter $ck_F = 5$ is taken as obtained from the FS in-plane topology extracted out of the AMRO experiment [6]. In many other compounds the FS consists of either multiple cylinders or a combination of a cylinder and a pair of corrugated planar sheets. Therefore, calculations introduced here can be used to obtain the field and angular behaviour of the wave amplitude in such systems as well.

### 4.1. ANGULAR OSCILLATIONS OF THE ACOUSTIC WAVE AMPLITUDE-INFLUENCE OF THE MECHANICAL AND THERMAL BOUNDARY

In organic conductors, qualitatively new phenomena, associated with extremely high electronic anisotropy, in particular related to the field orientation, have been found. Periodic oscillations of the kinetic and thermoelectric coefficients emerging when a constant magnetic field is turned from the direction normal to conducting layers toward the plane of the layers are characteristic of layered organic conductors and do not occur in ordinary metals. Since the behaviour of the thermally generated acoustic waves is determined by the coefficients that determine the transport in the conductor, acoustic angular oscillations are also expected to emerge when the field is rotated away from the normal with respect to the layers.

Shown in Fig. 1 are the low temperature angular oscillations of the acoustic wave amplitude in case of a *fixed* and *free* mechanical boundary, respectively. Presented are isothermal and adiabatic wave amplitudes at temperature $T$ = 20 K. In the following we compare the influence of boundary conditions, both mechanical and thermal, on the generation of bulk acoustic waves in organic conductors in order to estimate the efficiency of the linear thermoacoustic generation.

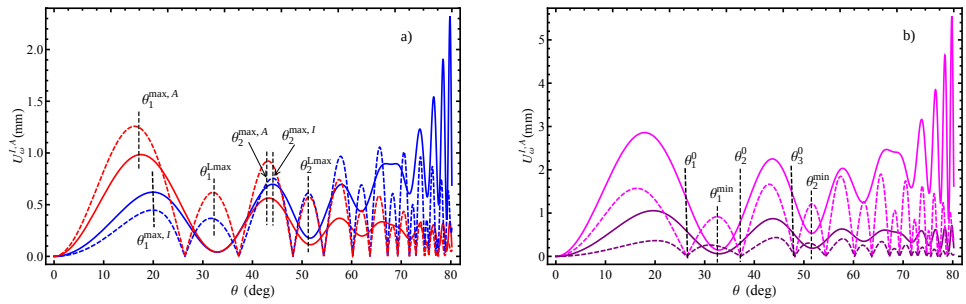


Fig. 1 – (Color online). Angular oscillations of the acoustic wave amplitude $U_\omega^{I,A}(\theta)$ at $T$=20 K for a) fixed isothermal (blue curves) and adiabatic (red curves) boundary, b) free isothermal (magenta curves) and adiabatic (purple curves) boundary. Solid curves represent the acoustic wave amplitude oscillations at $B = 3$ T and dashed curves are for $B = 8$ T, respectively. The regular periodic angular oscillations are seen at low fields ($B = 3$ T) and the existence of local maxima in both isothermal and adiabatic amplitude is evident at high fields ($B = 8$ T). The angular positions of the maxima (main $\theta_n^{\max}$ and local $\theta_n^{L\max}$), minima $\theta_n^{\min}$ and amplitude zeros $\theta_n^0$ are indicated.

We first note that in organic conductors a prominent acoustic wave generation manifests at angles up to $\theta \sim 80^\circ$. Exception are the angles for which field approaches the orientation close to the layers. This is because with tilting the field from the $z-$axis (that is normal to the layers and, hence, parallel to the axis of the Fermi cylinder) toward a direction parallel to the layers, the topology of the electron orbits in $\mathbf{k}$-space, which are always perpendicular to magnetic field $\mathbf{B}$, changes from

closed ($\theta < \pi/2$) to open ($\theta \approx \pi/2$). Since the existence of angular oscillations relies on the periodic electron motion on the closed orbits it is expected that they will be suppressed at angles close to the plane of the layers where closed orbits transform into a pair of open orbits. For $\beta - (\mathrm{BEDT-TTF})_2\mathrm{IBr}_2$ the characteristic angle when closed orbits change to open is estimated around $\theta \sim 80^\circ - 82^\circ$ [6], [7].

Figure 1 reveals strong dependence of the angular oscillations on the type of boundary. The wave amplitude is the largest for isothermal and free boundary at low fields in the whole range of angles. Although this makes the free boundary more preferable over the fixed one there are certain features that should be addressed concerning the angular behaviour of the wave amplitude with increasing field and angle. At low magnetic fields there are regular periodic oscillations whose amplitude increases or decreases with increasing angle, depending on the thermal condition, whereas at high fields the existence of local maxima in the angular dependence is evident for both isothermal and adiabatic case. More strikingly, we find that the amplitude for the isothermal fixed boundary becomes larger than the amplitude for the adiabatic one at $\theta > 40^\circ$ for $B = 3$ T and $\theta > 55^\circ$ for $B = 8$ T despite the absence of a heat flux through the conductor's surface in the latter. In the case of a free mechanical boundary the isothermal wave amplitude starts to increase with field at approximately the same angle where it becomes larger than the adiabatic one for the fixed boundary and exceeds the adiabatic wave amplitude in the whole range of angles. In addition, at high field and certain angles the wave amplitude for both thermal and mechanical boundary reaches a zero value, *i.e.*, the conductor is acoustically transparent. This can be more clearly seen from the $\tan\theta$ dependences plotted in Figs. 2 and 3. It is evident that at low fields ($B = 3$ T) the tendency is an increase of the isothermal wave amplitude $U_\omega^I$ and a decrease of the adiabatic wave amplitude $U_\omega^A$ with increasing angle for both mechanical boundaries (Fig. 2). At high fields ($B = 8$ T) different trends are apparent featuring the existence of local maxima and zero acoustic wave amplitude at certain angles (Fig. 3). Of note is that amplitude zeros, where the acoustic wave is maximally attenuated, are observed only at high fields whereas at low fields the amplitude is not strongly attenuated neither for isothermal nor for the adiabatic thermal boundary. This implies that other mechanisms could influence the thermoacoustic generation. The observed features indicate that at different thermal conditions the wave amplitude is conditioned by the angular behaviour of different transport coefficients that reflect the electron transport and dynamics in organic conductors for the geometry under consideration. These issues are discussed in detail below by studying the angular behaviour of the kinetic and thermoelectric coefficients that determine the wave amplitudes.

It is worth noting that we have also performed numerical integration of the integral solutions that we have obtained for the wave amplitude (eqs. 23, 24 and eqs. 26, 28) by using the expression for the heat source (eq. 31). We find that the

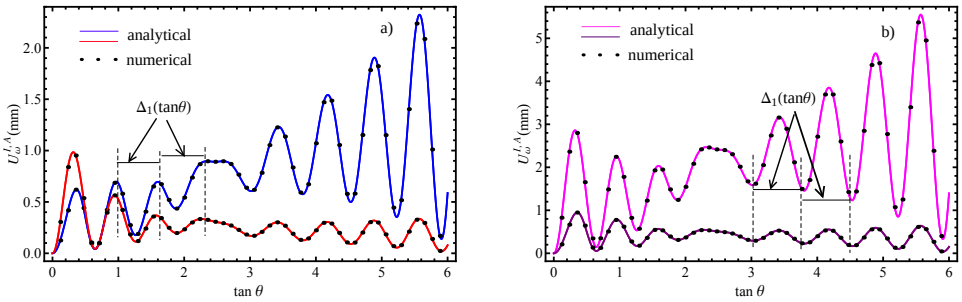


Fig. 2 – (Color online). $\tan\theta$ dependence of the acoustic wave amplitude $U_\omega^{I,A}(\tan\theta)$ for $T$=20 K and $B = 3$ T in the case of a) fixed and b) free mechanical boundary. The blue and magenta curves are for the isothermal case. Red and purple curves represent the adiabatic boundary. Solid curves represent the analytical calculations while the black dots are from the numerical integration of the wave amplitude. The period of oscillations $\Delta_1(\tan\theta)$ (see the text) is indicated.

numerical integration of the integral forms for the amplitude (black dots in Figs. 2 and 3) is a very good fit to the analytical calculations given by eqs. 33-35 (solid curves). This allows to safely use the integral forms for the amplitude derived in the present paper for further calculations and interpretation of different problems concerning the thermoacoustic generation.

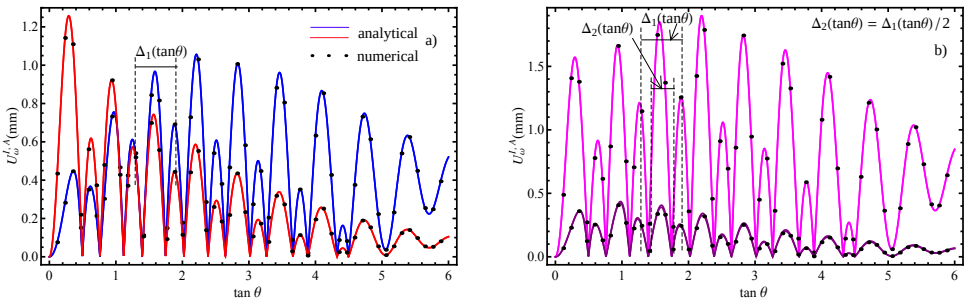


Fig. 3 – (Color online). $\tan\theta$ dependence of the acoustic wave amplitude $U_\omega^{I,A}(\tan\theta)$ for $T$=20 K and $B = 8$ T in the case of a) fixed and b) free mechanical boundary. The blue and magenta curves are for the isothermal case. Red and purple curves represent the adiabatic boundary. The local maxima are seen at each boundary condition up to $\tan\theta = 4.5$. The period of oscillations of the main maxima $\Delta_1(\tan\theta)$ and local maxima $\Delta_2(\tan\theta)$ is indicated.

The adiabatic wave amplitude is affected mainly by the thermoelectric coefficient $\alpha_{zx}$ while the isothermal wave amplitude involves, in addition to $\alpha_{zx}$, the in-plane conductivity $\sigma_{xx}$ that influences the flow of acoustic wave oscillations especially as the angle $\theta$ approaches the plane of the layers. For $ck_F \tan\theta \gg 1$ the positions of the main and local maxima as well as minima and amplitude zeros in the angular dependence of both acoustic wave amplitudes, $U_\omega^I$ and $U_\omega^A$, are around the

same angles. There is a slight shift between the angular positions of the first main maxima of the isothermal and adiabatic wave amplitude that appear at angles close to the direction perpendicular to the plane of the layers ($\theta_1^{\max} = 17.5^\circ - 20^\circ$) for both mechanical boundaries (Fig. 1) since for these angles the argument of Bessel functions is not much larger than unity ($ck_F \tan\theta = 1.6 - 1.8$). Because of this and additionally the existence of a heat flux through the isothermal boundary the electron drift velocity, $\bar{v}_z \simeq \frac{2t_c c}{\hbar} J_0(ck_F \tan\theta)$, along the acoustic wave at the first maximum is slightly different for the isothermal and adiabatic boundary. For the second main maxima around $\theta_2^{\max} = 43^\circ$ the shift is already negligible since $ck_F \tan\theta > 4$.

The angular positions of the wave amplitude are determined from the corresponding angular positions of the thermoelectric coefficient $\alpha_{zx}$. They are derived from the Bessel functions product $J_0(ck_F \tan\theta) J_1(ck_F \tan\theta)$ since for $ck_F \tan\theta \gg 1$ the first term in eq. (42) is dominant. Recalling that the Bessel functions can be approximated by $J_\nu(z) \approx \sqrt{\frac{2}{\pi z}} \cos\left(z - \frac{\nu\pi}{2} - \frac{\pi}{4}\right)$ for $z \gg 1$ one obtains the positions of the maxima and minima as well as amplitude zeros in the angular dependence of the acoustic wave amplitude. The main maxima in $U_\omega^{I,A}(\tan\theta)$ appear for $2ck_F \tan\theta - \pi = 2n\pi$ where $n = 0, 1, 2, 3, ...$ is an integer. It follows that the maximum amplitude is reached at angles $\theta_n^{\max}$ that satisfy the condition $\tan\theta_n^{\max} = \frac{\pi}{ck_F}(n + 1/2)$. The positions of the minima in the isothermal wave amplitude are obtained from $2ck_F \tan\theta - \pi = (2n+1)\pi$ and are found at angles $\theta_n^{\min}$ for which $\tan\theta_n^{\min} = \frac{\pi}{ck_F}(n+1)$. These angles also define the positions of the local maxima at $B = 8$ T as seen from Fig. 1. The amplitude zeros observed at high fields that separate the main and local maxima are found from $2ck_F \tan\theta - \pi = (2n+1)\pi/2$ and take place at angles $\tan\theta_n^0 = \frac{\pi}{2ck_F}(n+1/2)$. The maxima and minima in the angular dependences repeat with a same period $\Delta_1(\tan\theta) = \frac{2\pi\hbar}{cD_p}$ while the amplitude zeros are repeated at a half period, $\Delta_2(\tan\theta) = \frac{\pi\hbar}{cD_p}$. This allows to determine the FS diameter $D_p$ in the direction perpendicular to the vectors $\mathbf{q}$ and $\mathbf{B}$.

An important issue to emphasize is that the isothermal wave amplitude becomes larger than the adiabatic one at angles $\theta = \theta_{cr}$ such that $\tan\theta_{cr} \sim B/\sqrt{2}h$ for fixed while it is dominant over the adiabatic amplitude in the whole angular range for the free boundary. This is, however, not expected as there is no heat flux at the adiabatic thermal boundary. Our suggestion is that this kind of behavior is reflected only at low temperatures when the thermal skin depth $\delta_T$ is always larger than the electromagnetic $\delta_E$ and the thermal field dominates in the generation of acoustic oscillations over the electromagnetic one. There are several possibilities that could lead to that. First, at low $T$ the temperature distribution at the isothermal boundary $\Theta_I \sim 1/\delta_E$ is larger than the one at the adiabatic boundary $\Theta_A \sim 1/\delta_T$ since $\delta_T \gg \delta_E$. Second, the isothermal wave amplitude is conditioned by the in-plane electronic transport in addition to the interlayer transport (especially at the free boundary due to the no

fixed boundary condition at the surface for the wave amplitude) while the adiabatic one is mainly determined by the interlayer transport as evident from the equations (33-35). This is correlated with the increasing electron mean free path $l$ at lower temperatures and additionally the mean free path of the electrons in the plane of the layers is large as it is proportional to the Fermi velocity ($\bar{v}_x^{\max} = v_F$) whereas along the direction normal to the layers plane $l$ is much smaller since $\bar{v}_z^{\max} = \frac{2t_c}{\varepsilon_F} v_F$ (in $\beta - (\mathrm{BEDT} - \mathrm{TTF})_2\mathrm{IBr}_2$ the transfer integral $t_c$ is approximately $10^3$ times less than the Fermi energy $\varepsilon_F$). Third, in $\beta - (\mathrm{BEDT} - \mathrm{TTF})_2\mathrm{IBr}_2$ the conductivity $\sigma_{xx}$ within the layers is $10^3$ times larger than the interlayer one $\sigma_{zz}$ [1] indicating that for the isothermal boundary a larger number of charge carriers is involved in the transport that gives rise to the amplitude of acoustic oscillations.

Next we discuss the influence of the inductive mechanism on the thermoacoustic generation in organic conductors which exist in addition to the thermoelectric one in the presence of an external magnetic field. The inductive mechanism is due to the Lorentz force $\mathbf{F}_L = e(\mathbf{v} \times \mathbf{B})$ acting on the conduction electrons. At low fields the Lorentz force is smaller and the inductive mechanism does not affect the thermoacoustic generation strongly which is why the acoustic waves are not strongly attenuated at $B = 3$ T for both thermal and mechanical boundary (Fig. 1) but it is significant at high fields as evident from the existence of amplitude zeros at $B = 8$ T. This implies that at low fields the inductive mechanism does not exceeds the thermoelectric one but it is dominant at high fields for certain field orientations given by $\tan\theta_n^0 = \frac{\pi\hbar}{D_p}(n + 1/2)$. The inductive mechanism is the one responsible for appearance of local maxima in the acoustic wave angular oscillations at high fields. As charge carriers move across the FS under the influence of the magnetic field its component of velocity in a given direction will vary as it negotiates the various contours and corrugations (its total velocity remaining perpendicular to the FS at all times). Therefore, the angle between the electron velocity and the magnetic field also varies that leads to distinct action of Lorentz force on the conduction electrons and hence on the wave amplitude angular behavior. Provided the FS warping is very weak, $t_c \ll \varepsilon_F$, around the minima in the $U_\omega^{I,A}(\theta)$ dependence the electron velocities are nearly parallel to $\mathbf{B}$ at low field and the Lorentz force almost vanishes in this area, so that the electrons do not move on the FS, no matter whether they are situated on the small or big closed orbits. With increasing field the Lorentz force increases and is maximum when the electron velocity is perpendicular to $\mathbf{B}$, causing a maximum wave attenuation. That corresponds to the angles where amplitude zeros occur and therefore the minima that appear at low fields are now shifted towards smaller angles while at their angular positions local maxima emerge whose period of oscillations is half the period of oscillations of main maxima, $\Delta_2(\tan\theta) = \Delta_1(\tan\theta)/2$.

### 4.2. MAGNETIC FIELD DEPENDENCE OF THE ACOUSTIC WAVE AMPLITUDE

Figure 4 presents the amplitude of the thermally generated acoustic wave in the case of a *fixed* mechanical boundary as a function of a magnetic field for both isothermal and adiabatic thermal condition at $T$ = 20 K and several field directions from the normal to the layers that correspond to two peaks in the $U_\omega^{I,A}(\theta)$ dependence $\theta_2^{\max} = 43°$, $\theta_5^{\max} = 73°$ and for the first minimum/local maximum $\theta_1^{\min}$, $\theta_1^{L\max} = 32°$. Figure 5 presents the same in the case of a *free* mechanical boundary. Again, numerical integration with regards to magnetic field gives a good fit to the analytically obtained curves for the wave amplitude as seen from both figures.

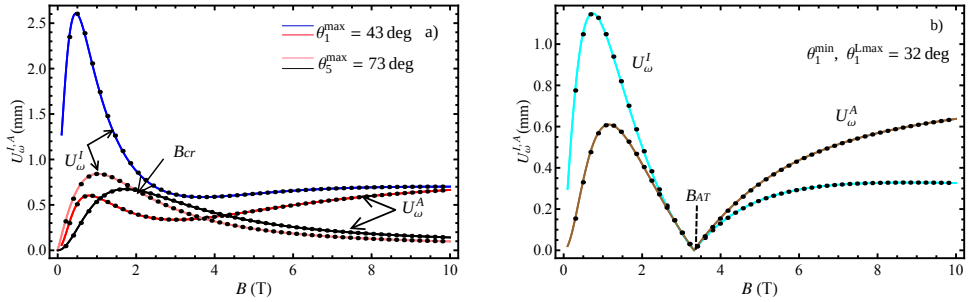


Fig. 4 – (Color online). Magnetic field dependence of the acoustic wave amplitude $U_\omega^{I,A}(B)$ for a fixed isothermal and adiabatic boundary at $T$=20 K and a) $\theta_2^{\max} = 43°$, $\theta_5^{\max} = 73°$, b) $\theta_1^{\min}$, $\theta_1^{L\max} = 32°$. Solid curves represent the analytical calculations while the black dots are from the numerical integration of the wave amplitude.

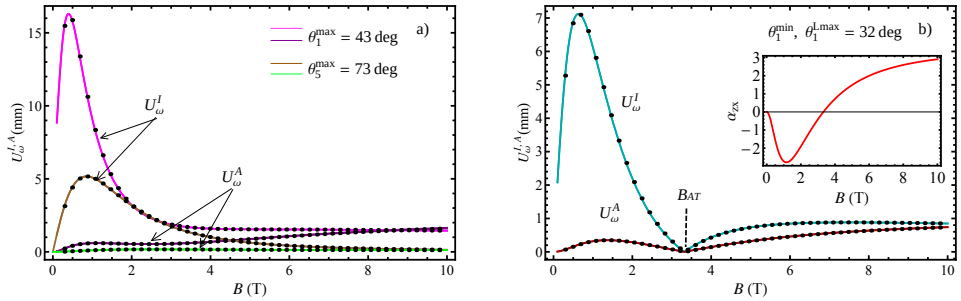


Fig. 5 – (Color online). Magnetic field dependence of the acoustic wave amplitude $U_\omega^{I,A}(B)$ in case of a free isothermal and adiabatic boundary at same $T$ and field directions from the normal to the layers as in Fig. 4. The inset in b) shows the magnetic field dependence of the thermoelectric coefficient $\alpha_{zx}$ at the same angle.

Magnetic field dependence reveals that the thermoacoustic generation is man-

ifested in a wide range of fields but with decreasing efficiency at high fields. The efficiency of the effect with field is significantly different depending on the angle between the magnetic field and normal to the layers, *i.e.*, if the angle corresponds to the maximum or minimum in the wave amplitude angular dependence. The thermoacoustic generation is significantly pronounced for the free mechanical boundary and different features are apparent in the wave amplitude behavior in consistency with the findings from the angular dependence. When the field is tilted at the main maxima the most effective thermoacoustic generation for isothermal fixed and free boundary is achieved at lower fields while the efficiency of the wave generation is almost constant with increasing field for the adiabatic thermal condition. As evident from Fig. 4a, if the angle $\theta$ corresponds to a field orientation away from the layers plane ($\theta = \theta_2^{\max} = 43^\circ$), the amplitudes $U_\omega^I(B)$ and $U_\omega^A(B)$ are decreasing after reaching a peak around $B = 0.5$ T while there is a steady increase for $B > 3$ T. As the field reaches close to the layers plane ($\theta = \theta_2^{\max} = 72.7^\circ$), the peak is shifted towards slightly higher field and both $U_\omega^I(B)$ and $U_\omega^A(B)$ are slowly decreasing with increasing field. Above $B_{cr} = 2$ T the adiabatic amplitude is slightly larger than the isothermal one indicating that at fields tilted close to the layers plane the influence of the in-plane electron transport is present only at lower fields. For a free boundary similar trends are apparent except that the isothermal amplitude is always larger than the adiabatic one (Fig. 5a) although quite opposite is expected due to the non-zero temperature distribution at the surface in the latter. It seems that a larger wave amplitude for the isothermal boundary is a common feature in organic conductors when the acoustic waves are thermally induced at low temperatures. This implies a possibility that the isothermal wave generation is conditioned, however, by the electromagnetic field in addition to the thermal field (especially in case of a free boundary because of the no fixed boundary condition (eq. 25)) while the adiabatic wave generation is solely due to the thermal field. Moreover, we see that the wave is not strongly attenuated with increasing field as in the case of high temperatures where it vanishes already at $B \sim 0.6$ T [2]. This is correlated not only with the weaker influence of the inductive mechanism but also with the weak coupling between the temperature and electromagnetic oscillations at low temperatures. Indeed, at low temperatures the skin depth of thermal field $\delta_T \sim\sqrt{\sigma_{zz}}$ is always larger than the one of electromagnetic field $\delta_E \sim 1/\sqrt{\sigma_{xx}}$ implying that the coupling between the temperature and electromagnetic oscillations is always weak and the acoustic waves are dragged into the conductor mainly by the thermal field. The electromagnetic skin depth in $\beta-(\mathrm{BEDT-TTF})_2\mathrm{IBr}_2$ crystals is of order $\delta_E = 0.12$ mm [8] while the thermal one would be around 10 times larger since $\sigma_{xx} \gg \sigma_{zz}$ allowing for the acoustic waves to propagate at large distance from the conductor's surface. This, in addition to the high quality of organic conductors would provide ultrasonic techniques to be used as a valuable tool in investigating electronic properties of these materials.

On the other hand, when the field is oriented at the minima (these are also the positions of the local maxima observed at high fields) the thermoacoustic generation is showing different behavior from the one seen at the main maxima featuring an acoustic transparency for both thermal and mechanical boundary at $B_{AT} = 3.3$ T for $\theta_1^{\min}$ and $\theta_1^{L\max}$ as seen in Figs. 4b and 5b. The field $B_{AT}$ is angle dependent increasing with rotating the field towards higher angular positions of the minima (local maxima). At this field the thermoelectric coefficient $\alpha_{zx}$ changes sign from negative to positive (inset in Fig. 5b) indicating a change in the sign of charge carries responsible for the thermoacoustic generation. Below $B_{AT}$ the electrons are involved in the acoustic wave generation whereas above $B_{AT}$ the process is conditioned by the holes. This provides an additional material for studying the properties of charge carriers in low dimensional conducting systems.

In recent decades the interest in investigations of electron phenomena in layered structures of organic origin rose considerably because of their great importance for applied sciences. Layered organic conductors are excellent objects for performing ultrasonic measurements due to the high crystal quality. Ultrasonic measurements on thermoacoustic generation would be a powerful tool for studying magnetic phase transition which is of particular interest for many of the conducting organic molecular crystals based on the BEDT-TTF and TMTSF molecules because they possess rich phase diagrams. Metallic, superconducting, and density wave phases are possible, depending on temperature, pressure, magnetic field, and anion type. It might be used to study the gap in the electronic structure as well as the inter- and in-plane electronic anisotropy in these materials arising from their complex structure. In addition, by studying the thermoacoustic generation in organic conductors with multilayered FS one can estimate the contributions from different groups of charge carriers in the effect for different polarization and direction of wave propagation. It may also be used to explain phonon interactions in the organic compounds as well as the acoustic energy absorption at high frequencies, where direct experimental measuring of the acoustic absorption coefficient to date is practically impossible.

## 5. CONCLUSIONS

The low temperature thermoacoustic bulk wave generation in an anisotropic organic conductor with quasi-two dimensional dispersion relation is considered using the Green's functions method. The solutions for both temperature distribution and acoustic wave amplitude are obtained in integral form that can be further used for deriving the corresponding analytical expressions as well as for numerically calculations for a given heat source at the conductor's surface. The method allows to comprehensively study the thermoacoustic generation in organic conductors by analysing the parameters that have a significant impact on the wave amplitude. The

angular oscillations which are characteristic only for the organic conductors and the magnetic field dependence of the wave amplitude are studied in detail. Specifically, the parameters for the organic conductor $\beta-(\mathrm{BEDT-TTF})_2\mathrm{IBr}_2$ are used to analyse the acoustic wave amplitude as it is an ideal model object demonstrating all the basic effects. We find that the amplitude exhibits many features associated with the quasi-two dimensionality of the energy spectrum. These include: larger isothermal than adiabatic amplitude at certain angles for the fixed and in whole angular range for the free mechanical boundary although there is a heat flux through the surface in the case of an isothermal condition; existence of local maxima and amplitude zeros at high fields; maximum efficiency of the thermoacoustic generation at low fields for each type of boundary; the wave generation is present at high fields as well except for certain fields $B_{AT}$ when the field is oriented at the minimum in the angular dependence. All of the observed features are studied and discussed in detail and represent a valuable tool for studying the electronic properties of layered organic conductors. In the organic conductor $\beta-(\mathrm{BEDT-TTF})_2\mathrm{IBr}_2$ the relaxation time of charge carriers $\tau$ is very small ($\tau$ = 10 ps) and thermoacoustic generation can be experimentally observed even at high frequencies of the heat source, $\omega = 10^8 - 10^9$ Hz, as the necessary condition $\omega\tau \ll 1$ is always fulfilled.

## REFERENCES


1. M. V. Kartsovnik, Chem. Rev. **104**, 5737–5781 (2004).
2. D. Krstovska, O. Galbova, T. Sandev, EPL **81**, 37006 (2008).
3. D. Krstovska, Int. J Mod. Phys. B **31**(3), 1750250 (2017).
4. D. Krstovska, B. Mitreska, Eur. Phys. J. B **90**, 249 (2017).
5. A. A. Abrikosov, "*Fundamentals of the theory of metals*", (2nd edn., North-Holland, Amsterdam, 1988).
6. M. V. Kartsovnik, V. N. Laukhin, S. I. Pesotskii, I. F. Schegolev, V. M. Yakovenko, J. Phys. I **2**, 89 (1992).
7. M. V. Kartsovnik, P. A. Kononovich, V. N. Laukhin, I. F. Schegolev, JETP Lett. **48**, 541 (1988).
8. A. Chernenkaya, A. Dmitriev, M. Kirman, O. Koplak, R. Morgunov, Solid State Phenomena **190**, 615 (2012).